Processible Nanostructured Materials with Electrical Conductivity and Magnetic Susceptibility: Preparation and Properties of Maghemite/Polyaniline Nanocomposite Films

Ben Zhong Tang,* Yanhou Geng,† Jacky Wing Yip Lam, and Bensheng Li‡

Department of Chemistry, Hong Kong University of Science & Technology (HKUST), Clear Water Bay, Kowloon, Hong Kong, China

Xiabin Jing, Xianhong Wang, and Fosong Wang

Changchun Institute of Applied Chemistry, Chinese Academy of Sciences (CAS), Changchun, Jilin 130022, China

A. B. Pakhomov and X. X. Zhang

Department of Physics, HKUST, Clear Water Bay, Kowloon, Hong Kong, China

Received January 13, 1999. Revised Manuscript Received March 22, 1999

We here present a versatile process for the preparation of maghemite/polyaniline (γ-Fe_2O_3/PAn) nanocomposite films with macroscopic processibility, electrical conductivity, and magnetic susceptibility. The γ-Fe_2O_3 nanoparticles are coated and the PAn chains are doped by anionic surfactants of ω-methoxypoly(ethylene glycol) phosphate (PEOPA), 4-dodecylbenzenesulfonic acid (DBSA), and 10-camphorsulfonic acid (CSA). Both the coated γ-Fe_2O_3 and the doped PAn are soluble in common organic solvents, and casting of the homogeneous solutions gives free-standing nanocomposite films with γ-Fe_2O_3 contents up to ~50 wt %. The morphology of the γ-Fe_2O_3 nanoparticles are characterized by transmission electron microscopy, UV−vis spectroscopy, and X-ray diffractometry. The γ-Fe_2O_3/PAn films prepared from chloroform/*m*-cresol solutions of DBSA-coated γ-Fe_2O_3 and CSA-doped PAn are conductive (σ = 82−237 S/cm) and superparamagnetic, exhibiting no hysteresis at room temperature. The zero-field-cooled magnetization experiment reveals that the nanocomposite containing 20.8 wt % γ-Fe_2O_3 has a blocking temperature (T_b) in the temperature region of 63−83 K.

Introduction

The development of nanocluster-based materials is a topic of great current interest.[1−3] Nanoclusters are ultrafine particles of nanometer dimensions located in the transition region between atoms and bulk solids. Quantum states in the nanoclusters are size-dependent, leading to novel mesoscopic properties that are sometimes dramatically different from those of the atomic and bulk counterparts.[4] Magnetic particles, for example, exhibit size effects.[5] Below a critical size, magnetic clusters become monodomain as opposed to multidomain in the bulk structure. Nanomagnets also show unusual phenomena such as superparamagnetism and quantum tunneling of magnetization. Because of the unique physical properties, magnetic nanoclusters have high potential for applications in diverse areas such as information storage,[6] color imaging,[7] magnetic refrigeration,[8] ferrofluids,[9] cell sorting,[10] medical diagnosis,[11] and controlled drug delivery.[12]

* To whom correspondence should be addressed.
† Present address: Max-Planck-Institut für Polymerforschung, Ackermannweg 10, Postfach 3148, 55021 Mainz, Germany.
‡ Present address: Department of Chemistry, Texas Christian University, 2800 S. University Drive, Fort Worth, TX 76129.

(1) (a) *Clusters*; special issue in *Science* **1996**, *271*. (b) *Nanostructured Materials*; special issue in *Chem. Mater.* **1996**, *8*.

(2) For reviews, see: (a) Beecroft, L. L.; Ober, C. K. *Chem. Mater.* **1997**, *9*, 1302. (b) Antonietti, M.; Goltner, C. *Angew. Chem., Int. Ed.* **1997**, *36*, 910. (c) Weller, H. *Angew. Chem., Int. Ed.* **1996**, *35*, 1079.

(3) (a) *Nanostructured Powders and Their Industrial Applications*; Beaucage, G., Ed.; Materials Research Society: Warrendale, PA, 1998. (b) *Nanophase and Nanocomposite Materials II*; Komarneni, S., Parker, J. C., Wollenberger, H. J., Eds.; Materials Research Socirty: Warrendale, PA, 1997. (c) *Nanostructured Materials*; Jena, P., Ed.; Nova Science: New York, 1996. (d) *Nanostructured Systems*; Reed, M., Ed.; Academic Press: Boston, 1992.

(4) (a) *Nanostructures and Quantum Effects*; Sakaki, H., Noge, H., Ed.; Springer-Verlag: Berlin, 1994. (b) Woggon, U. *Optical Properties of Semiconductor Quantum*; Springer-Verlag: Berlin, 1997.

(5) (a) *Nanomagnetism*; Hernando, A., Ed.; Kluwer Academic Publishers: Dordrecht, The Netherlands, 1993. (b) *Magnetic Properties of Fine Particles*; Dormann, J. L., Fiorani, D., Eds.; North-Holland: Amsterdam, 1992. (c) *Science and Technology of Nanostructured Magnetic Materials*; Hadjipanayis, G. C., Prinz, G. A., Eds.; Plenum Press: New York, 1991.

(6) Audram, R. G.; Huguenard, A. P. U.S. Patent 4 302 523, 1981.

(7) Ziolo, R. F. U.S. Patent 4 474 866, 1984.

(8) McMichael, R. D.; Shull, R. D.; Swartzendruber, L. J.; Bennett, L. H.; Watson, R. E. *J. Magn. Magn. Mater.* **1992**, *111*, 29.

(9) Rosensweig, R. E. *Ferrohydrodynamics*; MIT Press: Cambridge, 1985.

(10) Pope, N. M.; Alsop, R. C.; Chang, Y.-A.; Sonith, A. K. *J. Biomed. Mater. Res.* **1994**, *28*, 449.

10.1021/cm9900305 CCC: $18.00
Published on Web 05/07/1999

To realize the full potential of the attractive technological applications, it is highly desirable to endow the magnetic nanoclusters with processibility. Because of the excellent tractability of polymeric materials, much research effort has been directed toward the development of methodologies and processes for the incorporation of magnetic nanoclusters into polymeric matrixes.[13,14] Of particular interest is the integration of magnetic nanoclusters with conducting polymers because the resulting nanocomposites may possess unique magnetic, electrical, and optical properties. Such nanomaterials are expected to find applications in electromagnetic interference shielding,[15] electrochromic devices,[16] sensing and actuating technologies,[13d,17] nonlinear optical systems,[18] and molecular engineering of nanomotors.[19]

The attempts in the preparation of nanomagnet-containing conducting polymers, however, have met with only limited success.[20] Nguyen and Diaz polymerized sodium pyrrole-*N*-propylsulfonate (PyS) in the presence of $FeCl_3$ and converted the polymerization product into γ-Fe_2O_3/poly(PyS) by oxidation.[21] The resulting black powdery nanocomposites, however, were insoluble and insulating ($\sigma = 3.4 \times 10^{-7}$ S/cm). Bidan et al. used an electropolymerization technique to embed "chelating ligand"-coated γ-Fe_2O_3 nanoparticles in polypyrrole (PPy).[22] The electrical conductivity values of the γ-Fe_2O_3/PPy nanocomposites were in the range of 0.026−1.9 S/cm, which are far below those (100−600 S/cm) of the parent PPys doped by ASF_6^-, BF_4^-, and I_3^-.[23] Wan and co-workers prepared magnetite/polyaniline (Fe_3O_4/PAn) nanocomposites by mixing aqueous solutions of iron(II) sulfate and 1-methyl-2-pyrrolidinone (NMP) solutions of PAn at different pH values.[24] The powdery precipitate obtained from the acidic conditions (e.g., at pH = 1) contained a low concentration of Fe_3O_4 nanoparticles (as low as ~0.01%)[25] and had electrical conductivity as low as $\sim 10^{-4}$ S/cm. The precipitate obtained from the basic conditions (e.g., at pH = 14) contained more Fe_3O_4 nanoparticles but was electrically completely insulating.

Chart 1

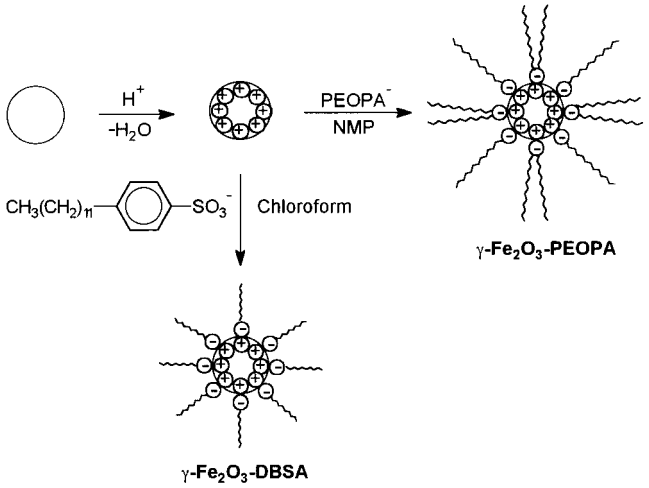

Thus the development of macroscopically processible nanocomposites with usefully high electrical conductivity and magnetic susceptibility remains a challenge and demands careful design. The conducting polymer matrixes to be used, for example, must be *soluble* and *stable*, especially in their doped states (although the opposite is unfortunately often true for many conjugated polymers[26,27]). The doping of the polymers by protonation of strong inorganic acids such as HCl should be carefully avoided because the harsh acids disintegrate the nanostructured magnetic clusters.[13c,25] In this work, we developed a process for the preparation of γ-Fe_2O_3/PAn nanocomposite films. We employed anionic surfactants to coat γ-Fe_2O_3 nanoparticles (Chart 1) and to dope PAn chains (Chart 2). Both the coated γ-Fe_2O_3 nanoparticles and the doped PAn emeraldine salts are soluble in common organic solvents, giving stable solutions that can be readily processed into large-area thin films by macroscopic techniques such as static casting and spin coating. The resultant γ-Fe_2O_3/PAn nanocomposite films are free-standing, possess high electrical conductivity (82−237 S/cm), and show superparamagnetism.

Experimental Section

Materials. The PAn samples were synthesized by our previously published procedures.[28] Poly(ethylene glycol) methyl

(11) Marchessault, R. H.; Richard, S.; Rioux, P. *Carbohydr. Res.* **1992**, *224*, 133.
(12) Bhatnagar, S. P.; Rosensweig, R. E. *J. Magn. Magn. Mater.* **1995**, *149*, 198.
(13) (a) Sohn, B. H.; Cohen, R. E. *Chem. Mater.* **1997**, *9*, 264. (b) Chen, L.; Yang, W.-J.; Yang, C.-Z. *J. Mater. Sci.* **1997**, *32*. 3571. (c) Kommareddi, N. S.; Tata, M.; John, V. T.; Mcpherson, G. L.; Herman, M. F.; Lee, Y.-S.; O'Connor, C. J.; Akkara, J. A.; Kaplan, D. *Chem. Mater.* **1996**, *8*, 801. (d) Klapcinski, T.; Galeski, A.; Kryszewski, M. *J. Appl. Polym. Sci.* **1995**. *58*, 1007. (e) Gao, M.; Peng, X.; Shen, J. *Thin Solid Films* **1994**, *248*, 106.
(14) (a) Kroll, E.; Winnik, F. M.; Ziolo, R. F. *Chem. Mater.* **1996**, *8*, 1594. (b) Vassiliou, J. K.; Mehrotra, V.; Russell, M.; McMichael, R. D.; Shull, R. D.; Ziolo, R. F. *J. Appl. Phys.* **1993**, *73*, 5109. (c) Ziolo, R. F.; Giannelis, E. P.; Weinstein, B. A.; O'Horo, M. P.; Ganguly, B. N.; Mehrotra, V.; Rusell, M. W.; Huffman, D. R. *Science* **1992**, *257*, 219.
(15) Miyauchi, S.; Abiko, H.; Sorimashi, Y.; Tsubata, I. *J. Appl. Polym. Sci.* **1989**, *37*, 289.
(16) Shen, P. K.; Huang, H. T.; Tseung, A. C. C. *J. Electrochem. Soc.* **1992**, *139*. 1840.
(17) Gandhi, M. V.; Thomspon, B. S. In *Smart Materials and Structures*; Chapman & Hall: London, 1992.
(18) (a) Peng, X.; Zhang, Y.; Yang, J.; Zou, B.; Xiao, L.; Li, T. *J. Phys. Chem.* **1992**, *96*, 3412. (b) Zou, B. S.; Zhang, Y.; Xiao, L. Z.; Li, T. J. *Chin. J. Semicond.* **1991**, *12*, 145.
(19) Tang, B. Z.; Xu, H. *Macromolecules* **1999**, *32*, 2569.
(20) For a review, see: Kryszewski, M.; Jeszka, J. K. *Synth. Met.* **1998**, *94*, 99.
(21) Nguyen, T.; Diaz, A. *Adv. Mater.* **1994**, *6*, 858.
(22) (a) Bidan, G.; Jarjayes, O.; Fruchart, J. M.; Hannecart, E. *Adv. Mater.* **1994**, *6*, 152. (b) Jarjayes, O.; Auric, P. *J. Magn. Magn. Mater.* **1994**, *138*, 115. (c) Jarjayes, O.; Fries, P. H.; Bidan, G. *Synth. Met.* **1995**, *69*, 343.
(23) Frommer, J. E.; Chance, R. R. In *Encyclopedia of Polymer Science and Engineering*; Kroschwitz, J. I., Ed.; Wiley: New York, 1990.
(24) (a) Wan, M.; Li, W. *J. Polym. Sci. Polym. Chem.* **1997**, *35*, 2129. (b) Wan, M.; Zhou, W.; Li, J. *Synth. Met.* **1996**, *78*, 27.
(25) The low Fe_3O_4 content of the nanocomposite is probably due to the dissolution of the iron oxide in the strong acid of HCl: (a) Cotton, F. A.; Wilkinson, G. *Advanced Inorganic Chemistry*, 5 th ed.; Wiley: New York, 1988. (b) Kobayazhi, Y.; Kawashima, D.; Tomita, A. *Chem. Mater.* **1997**, *9*, 1887. (c) Miyoshi, H.; Yoneyama, H. *J. Chem. Soc., Faraday Trans. 1* **1989**, *85*, 1873.
(26) (a) *Handbook of Conducting Polymers*, 2nd ed.; Skotheim, T. A., Elsenbaumer, R. L., Reynolds, J. R., Eds.; Marcel Dekker: New York, 1998. (b) *Conjugated Polymers and Related Materials: the Interconnection of Chemical and Electronic Structure*; Salaneck, W. R., Lunstrom, I., Ranby, B., Eds.; Oxford University Press: Oxford, 1993. (c) *Conjugated Conducting Polymers*; Kiess, H, G., Ed.; Springer-Verlag: Berlin, 1992. (d) *Conjugated Polymers*; Breads, J. L., Silbey, R., Eds.; Kluwer: Dordrecht, The Netherlands, 1991.
(27) Masuda, T.; Tang, B. Z.; Higashimura, T.; Yamaoka, H. *Macromolecules* **1985**, *18*, 2369.

Chart 2

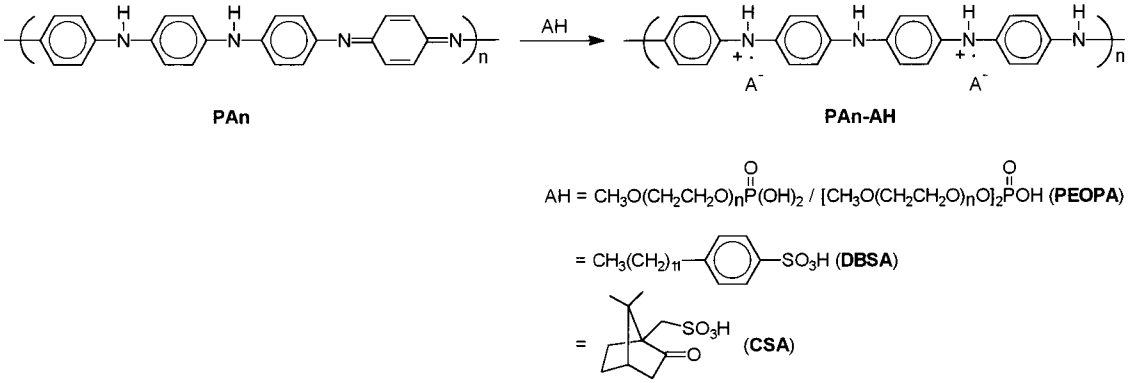

ether (M_n ~550; Aldrich), 4-dodecylbenzenesulfonic acid (DBSA; Kanto Chemical), and 10-camphorsulfonic acid (CSA; Aldrich) were dried at 40 °C in vacuo for prolonged time prior to use. Water was double distilled. All other reagents and solvents including iron(II) chloride tetrahydrate, iron(III) chloride, phosphorus pentoxide (P_4O_{10}; named *pentoxide* for historical reasons[29]), ammonium hydroxide (30% NH_3 in water), triethylamine, benzene, chloroform, *m*-cresol, tetrahydrofuran (THF), and NMP were purchased from Aldrich and used as received.

Synthesis of γ-Fe_2O_3 Nanoparticles. The nanoparticles were prepared according to published procedures[30] with some modifications. In a typical run, 1.99 g of $FeCl_2 \cdot 4H_2O$ (10.0 mmol) and 3.25 g of $FeCl_3$ (20.0 mmol) were dissolved respectively in 10 and 20 mL of water. The two iron−salt solutions were combined and dropped into 200 mL of 0.6 M aqueous ammonia solution in 20 min with vigorous stirring. The pH values of the reaction mixture were kept in the range of 11 to 12 with the addition of a concentrated ammonium hydroxide solution. The resulting nanoparticles were separated by centrifugation (MSE Mistral 1000) and washed with distilled water three times. The nanoparticles were further washed with THF three times and then dried in air for prolonged time in a warm oven.

Synthesis of ω-Methoxypoly(ethylene glycol) Phosphates (PEOPA). The phosphate surfactant was prepared by the reaction of poly(ethylene glycol) methyl ether with phosphorus pentoxide by a well-known reaction procedure.[29] Into a benzene solution (50 mL) of phosphorus pentoxide (5.2 g, 18 mmol) was added dropwise 50 mL of poly(ethylene glycol) methyl ether (55.0 g, 100 mmol). The mixture was refluxed under nitrogen for 2 h. The unreacted phosphous pentoxide was removed by filtration. Removal of the solvent by distillation gave colorless and transparent PEOPA surfactant.

Coating of γ-Fe_2O_3 Nanoparticles with Anionic Surfactants. The nanoparticles were coated with PEOPA and DBSA in different conditions (cf., Chart 1). Typical examples for the preparation of the surfactant-coated nanoparticles are as follows:

1. γ-Fe_2O_3−PEOPA. Into a solution of PEOPA (5 drops) in NMP (13 mL) was added a small amount of dry γ-Fe_2O_3 nanoclusters with stirring. Large particles of the nanoclusters were removed by centrifugation at 2500 rpm for 20 min, giving a stable solution with a γ-Fe_2O_3 concentration of 0.78%.

2. γ-Fe_2O_3−DBSA. A small amount of the γ-Fe_2O_3 nanoclusters were added into a solution of DBSA (1.5 g) in 25 mL of chloroform. After the large particles of the nanoclusters were removed by centrifugation at 2500 rpm for 20 min, a stable solution with a γ-Fe_2O_3 concentration of 3.43% was obtained.

Preparation of Surfactant-Doped PAn Solutions. The solutions of the PAns doped with different kinds and amounts of surfactants were prepared in different concentrations (cf., Chart 2). Typical examples for the preparation of the PAn-surfactant solutions are as follows:

1. PAn−PEOPA. PAn (0.4 g) was gradually added into 20 mL of NMP under stirring. After the PAn was dissolved, 1.6 g of PEOPA was added, and the resultant solution was filtered before use.

2. PAn−DBSA. PAn (0.5 g) and DBSA (2.2 g; *must be predried*) were thoroughly mixed in the solid state by grinding in a smooth agate mortar in an inert-atmosphere glovebox (Vacuum Atmosphere VAC MO-20). The PAn−DBSA solid mixture was added into 10 mL of chloroform. A homogeneous solution formed after 24-h stirring.

3. PAn−CSA. PAn (0.3 g) and CSA (0.4 g) were thoroughly mixed. The mixture was added into 20 mL of chloroform/*m*-cresol (4:6 by volume), and a homogeneous solution was obtained after 24-h stirring.

Preparation of γ-Fe_2O_3/Polyaniline Nanocomposite Films. Quantitative amounts of the NMP solutions of γ-Fe_2O_3−PEOPA and PAn−PEOPA were combined with stirring. The resulting solutions were cast onto glass plates. Controlled evaporation of the solvent by heating the solutions with an IR lamp gave free-standing γ-Fe_2O_3−PEOPA/PAn−PEOPA nanocomposite films. Similarly, different amounts of the chloroform solutions of γ-Fe_2O_3−DBSA were slowly added into the chloroform solutions of PAn−DBSA with stirring, but gels formed during the addition processes. No gelation occurred when the chloroform solutions of γ-Fe_2O_3−DBSA were admixed with the chloroform/*m*-cresol solutions of PAn−CSA, and static casting of the resulting homogeneous solutions at room temperature gave the desired γ-Fe_2O_3−DBSA/PAn−CSA nanocomposite films with different γ-Fe_2O_3 contents.

Characterization. To determine the γ-Fe_2O_3 concentration of a surfactant-coated nanoparticle solution, triethylamine was added to the solution to strip the coating on the surfaces of the nanoparticles. The decoated nanoparticle precipitate was filtered, washed, dried, and weighed. The γ-Fe_2O_3 concentration was estimated using the following equation:

$$\gamma\text{-}Fe_2O_3 \text{ concentration (wt \%)} = (W_p/W_t) \times 100 \quad (1)$$

where W_p is the weight of the nanoparticle precipitate and W_t is the total weight of the solution.

Morphology of the γ-Fe_2O_3 nanoparticles was investigated by a JEOL JEM-2010 high-resolution (down to 0.18 nm) transmission electron microscope (TEM) operating at an accelerating voltage of 200 kV. The samples for the TEM analysis were prepared by dispersing the nanoparticles in ethanol and then dropping the resultant suspension onto the carbon-coated copper microgrids. Electronic absorption spectra of the nanoparticles dispersed in chloroform and water were measured on a Milton Roy Spectronic 3000 array spectrometer.

(28) (a) Geng, Y.; Li, J.; Sun, Z.; Jing, X.; Wang, F. *Synth. Met.* **1998**, *96*, 1. (b) Geng, Y.; Jing, X.; Wang, F. *J. Macromol. Sci.-Phys.* **1997**, *36B*, 125.

(29) (a) Reference 25a, p 400. (b) Walker, B. J. *Organophosphorous Chemistry*; Penguin Books: Baltimore, 1972. (c) *Phosporous Chemistry*; Walsh, E. N., Griffith, E. J., Parry, R. W., Quin, L. D., Eds.; ACS Symposium Series 486; American Chemical Society: Washington, DC, 1992.

(30) Zhang, L.; Papaefthymiou, G. C.; Ying, J. Y. *J. Appl. Phys.* **1997**, *81*, 6892. (b) Kang, Y. S.; Risbud, S.; Rabolt, J. F.; Stroev, P. *Chem. Mater.* **1996**, *8*, 2209. (c) Mørup, S.; Mødker, F.; Hendriksen, P. V.; Linderoth, S. *Phys. Rev. B* **1995**, *52*, 287.

X-ray diffraction (XRD) diagrams of the γ-Fe_2O_3/PAn nanocomposites and the parent γ-Fe_2O_3 and PAn powders were recorded on a Philips PW 1830 powder diffractometer using the monochromatized X-ray beam from the nickel-filtered Cu $K\alpha$ radiation. Average diameters of the γ-Fe_2O_3 nanocrystals (D; Å) were estimated using Scherrer equation:

$$D = k\lambda/\alpha \cos\theta \quad (2)$$

where k is the shape factor, λ is the X-ray wavelength (1.5406 Å), α is the full width at half-maximum (fwhm) expressed in unit of 2θ, and θ is the Bragg angle (deg).

Electrical conductivity (σ) of the doped PAn and γ-Fe_2O_3/PAn nanocomposite films was measured by standard four-probe method.[28] Magnetization measurements were performed using a superconducting quantum interference device (SQUID) magnetometer (Quantum Design MPMS-5S) at fields ranging from 0 to 16 kOe and at temperatures ranging from 1.8 to 300 K. For zero-field-cooled (ZFC) magnetization, the sample was cooled to 1.8 K with the magnetic field set to zero. After stabilization at the low temperature for ~15 min, a weak magnetic field of 50 Oe was applied, and the magnetization was measured while the temperature was increased. The system was allowed to equilibrate before each measurement. In the field-cooled (FC) experiments, the sample was cooled to 5 K with the weak magnetic field of 50 Oe applied. The magnetization was measured while stepping the temperature up to 300 K. The blocking temperature (T_b) was estimated from the temperature at which the ZFC magnetization curve shows a peak maximum (T_{max}) using the following equation:[22b,30c]

$$T_{max} = \beta T_b \quad (3)$$

where β is a constant related to the size distribution of the particles.

Results and Discussion

Synthesis of γ-Fe_2O_3 Nanoparticles. The preparation of iron oxides from aqueous solutions of iron salts involves a complex process of multiple steps including deprotonation, hydrolysis, oxidation, precipitation, nucleation, crystallization, dehydroxylation, and/or dehydration.[25a,31] It is known that precipitation of pure Fe^{3+} ions typically produces amorphous hydrated oxyhydroxide that is easily converted to α-Fe_2O_3 of the corundum structure where the oxide ions form a hexagonally close-packed array with all the Fe^{3+} ions occupying octahedral interstices. Because of the stronger preference of Fe^{2+} ions for octahedral interstices than Fe^{3+} ions, introduction of Fe^{2+} ions in the crystallization promotes the formation of γ-Fe_2O_3 of the cation-deficient spinel structure of the $A[B_2]O_4$ type in which some of the Fe^{3+} ions occupy tetrahedral interstices.[32] Thus, in the synthesis of the iron oxide nanoparticles, we used an iron salt mixture of $FeCl_3$ and $FeCl_2$ with an Fe^{3+}/Fe^{2+} ratio of 2 to facilitate the packing of the iron cations in the spinel structure of γ-Fe_2O_3.[30]

Figure 1 shows the TEM micrographs of the γ-Fe_2O_3 nanoparticles. The particles are almost spherical in shape with an average diameter of ~10 nm. The crystalline nature of the nanoparticles are confirmed by their electron diffraction patterns. The nanoparticles

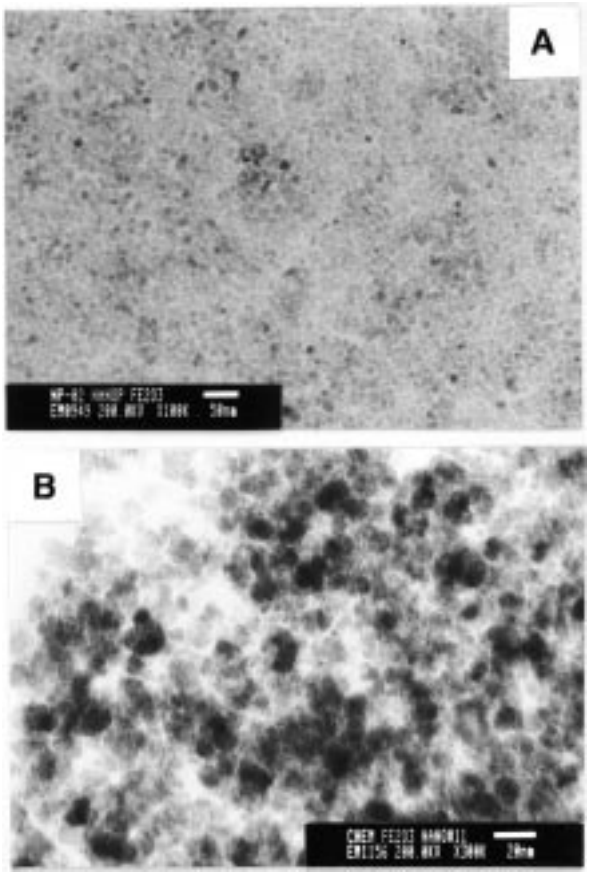

Figure 1. Transmission electron micrographs of γ-Fe_2O_3 nanoparticles taken at magnifications of (A) 100 000 and (B) 300 000. Scale bar (nm): (A) 50 and (B) 20.

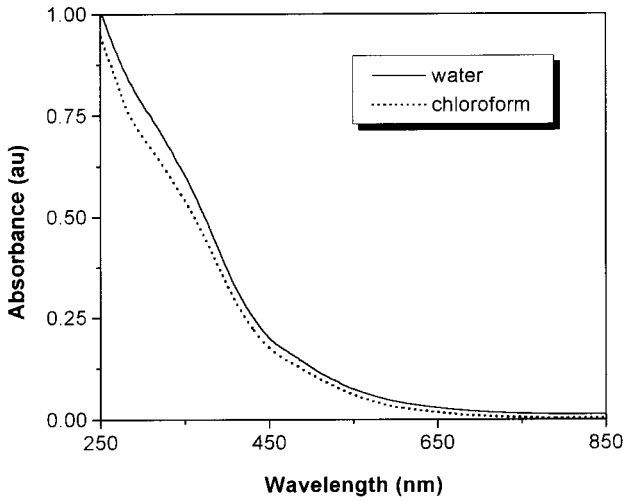

Figure 2. UV−vis absorption spectra of γ-Fe_2O_3 nanoparticles dispersed in chloroform and water.

dispersed in both water and chloroform absorb little in the visible spectral region (Figure 2), in accordance with their nanometer size and demonstrative of their optical transparency.

Before being incorporated into the polymer matrix, the nanoparticles are coated by surfactant molecules with the aims of (i) increasing their solubility in organic solvents, (ii) shielding them from the attack of the dopants of the conducting polymers, (iii) preventing them from aggregating during the film preparation, (iv) improving their miscibility with organic polymers, and

(31) Jambor, J. L.; Dytrizac, J. E. *Chem. Rev.* **1998**, *98*, 2549. (b) Schwertmann, U.; Cornell, R. M. *Iron Oxides in Laboratory*; VCH: New York, 1991. (c) Schwertmann, U.; Murad, E. *Clays Clay Minerol.* **1983**, *31*, 277.

(32) Tronc, E.; Jolivert, J. P. In *Nanophase Materials*; Hadjipanayis, G. C., Siegel, P. W., Eds.; Kluwer: Dordrecht, The Netherlands, 1994; p 21.

(v) enhancing the quality of the resultant nanocomposite films. The nanoparticles are prepared under basic conditions (pH = 11−12), and their surfaces are thus negatively charged with the oxygen ions located on the outermost shells.[20,30a] The negative charge can also be from the hydroxy groups due to the incomplete conversion of the $Fe(OH)_x$ and/or FeO(OH) species to γ-Fe_2O_3.[14c,31] Such negatively charged nanoparticles readily dissolve in strong mineral acids.[25] In our preliminary experiments, we attempted to dope polyaniline and substituted polyacetylenes containing naked (uncoated) nanoparticles of γ-Fe_2O_3 by HCl but found that most of the iron oxide particles were destroyed.[33] Kang et al. have used very dilute solutions of HCl (0.01 M) to neutralize the anionic charges on the surfaces of their iron oxide nanoparticles, which generates cationic colloidal nanoclusters.[30b] In our case, the large amount of HCl necessary for doping the conjugated polymer matrixes continuously erodes the nanoparticle surfaces by converting the iron oxide to water-soluble iron chloride species, thus leaving little quantity of the nanomagnet particles in the polymer matrixes. The nanoparticles, however, survive the organic acids (anionic surfactants) of PEOPA and DBSA used in this study. When the nanoparticles are added into a dilute solution of PEOPA, the phosphorous acid reacts with the basic shells of the nanoparticles. The protons of the acid combine with oxygen ions and/or hydroxy groups on the surfaces of the nanoparticles, releasing water molecules (cf., Chart 1). The oxygen-deficient shells are positively charged, and the negatively charged phosphate ions are attracted by the shells via ionic interaction, thus coating the nanoparticles in a micelle-like fashion. Similarly, the nanoparticles can be coated by the anionic surfactant of DBSA.

Preparation of γ-Fe_2O_3/Polyaniline Nanocomposites. The polymer matrix for hosting the nanoparticles must meet the following, among other, primary requirements: soluble, stable, and conductive. PAn has often been referred to as one of the most promising conducting polymers for commercialization.[35] PAn is easy to prepare (straightforward polymerization with high yield)[28] and is inexpensive. Most importantly, especially to this project, the doped PAn is readily soluble, chemically stable (e.g., highly resistant to air oxidation), and electrically conductive.[24a,36,37] In this work, we chose PAn as the conducting polymer matrix and doped it with the anionic surfactants PEOPA, DBSA, and CSA (cf., Chart 2). The doping is realized by the protonation of the imine nitrogen of the emeraldine base, which confers positive charges on the polymer chain.[38] The positive charges are balanced by the anionic parts of the acids, and the effective wrapping of the cationic PAn chains by the surfactant counterions makes the emeraldine salts readily soluble in common solvents.

The solubilization power of the three surfactants, however, are quite different. Only about half mole amount of PEOPA is needed to help solubilize PAn in NMP, possibly due to the efficient wrapping and strong plasticization effects of the oligomeric PEO chains. At least equal mole amount of DBSA, however, must be used in order to solubilize PAn.[36,39] Moreover, the DBSA must be predried and thoroughly mixed with PAn in the solid state under an atmosphere of dry nitrogen because water acts as a coagulant in the PAn−DBSA system, inducing undesirable gel formation.[39a,40] While water still needs to be excluded, much less amount (about 50 mol %) of CSA is required to ensure the complete dissolution of PAn in chloroform/*m*-cresol mixtures with the volume ratios ranging from 6:4 to 4:6, presumably due to the well-advocated molecular recognition effects.[37,39a,41]

Both the coated γ-Fe_2O_3 and the doped PAn are soluble in common solvents, enabling the fabrication of the nanocomposite films by simple static casting of the nanoparticle/polymer solutions. When the γ-Fe_2O_3 nanoparticles are coated and the PAn chains are doped by the PEOPA surfactant, ductile PAn films with γ-Fe_2O_3 contents as high as >50% (relative to PAn) can be readily prepared from their NMP solutions, thanks to the plasticization effect of the long, flexible PEO chains. However, when the chloroform solutions of the DBSA-coated γ-Fe_2O_3 and DBSA-doped PAn are admixed, gels always form in the early stage of the mixing processes. The reason for the gelation is not clear at present. One possibility is that the acidity of the nanoparticle solutions increases upon their addition into the polymer solutions where a large amount of BSA acid exists (vide supra). Part of the free acid molecules that are not bonded to or complexed with the PAn chains may have reacted with the iron oxide nanoparticles, which generates water, a coagulator for the PAn−DBSA system.[39a,40] The gelation problem makes it difficult, if not impossible, to fabricate uniform films from the chloroform solutions of γ-Fe_2O_3−DBSA and PAn−DBSA.

No gels form when the chloroform solutions of DBSA-coated γ-Fe_2O_3 are added dropwise into the chloroform/*m*-cresol solutions of CSA-doped PAn, probably because much less amount of CSA is used to dope PAn and all of the CSA molecules are strongly bonded to the PAn chains via the molecular recognition mechanism.[37,39a,41] Free-standing γ-Fe_2O_3−DBSA/PAn−CSA nanocomposite films with γ-Fe_2O_3 contents up to ∼50% can be readily prepared by the controlled evaporation of the solvents of the mixture solutions cast on glass plates at room temperature. The films are strong and tough,

(33) Li, B.; Tang, B. Z. *Proc. Symp. Front. Chem.* **1997**, 468. (b) Cheuk, K. L.; Li, B.; Lam, J. W. Y.; Tang, B. Z. Unpublished results.
(34) Meldrum, F. C.; Kotov, N. A.; Fendler, J. H. *J. Phys. Chem.* **1994**, *98*, 4506.
(35) Innis, P. C.; Norris, I. D.; Kane-Maguire, L. A. P.; Wallace, G. G. *Macromolecules* **1998**, *31*, 6521. (b) Turyan, I.; Mandler, D. *J. Am. Chem. Soc.* **1998**, *120*, 10733. (c) Wei, Y.; Yeh, J.-M.; Jin, D.; Jia, X.; Wang, J.; Jang, G.-W.; Chen, C.; Gumbs, R. W. *Chem. Mater.* **1995**, *7*, 969. (d) Wei, Y.; Hsueh, K. F.; Jang, G.-W. *Macromolecules* **1994**, *27*, 518. (e) Gennis, E. M.; Boyle, A.; Lapkowski, M.; Tsintavis, C. *Synth. Met.* **1990**, *36*, 139. (f) Allied-Signal, for example, started to commercialize PAn under the tradename of Versicon in the early 1990s.
(36) Cao, Y.; Smith, P.; Heeger, A. J. *Synth. Met.* **1992**, *48*, 91.
(37) Stejskal, J.; Sapurina, I.; Trchova, M.; Prokes, J.; Krivka, I.; Tobolkova, E. *Macromolecules* **1998**, *31*, 2218.
(38) Geng, Y.; Jing, X.; Li, J.; Wang, F. *Macromol. Rapid Commun.* **1997**, *18*, 73. (b) Wang, L.; Jing, X.; Wang, F. *Synth. Met.* **1989**, *29*, E363. (c) Stafstrom, S.; Biedas, J. L.; Epstein, A. J.; Woo, H. S.; Tanner, D. B.; Huang, W. S.; MacDiarmid, A. G. *Phys. Rev. Lett.* **1987**, *59*, 1464.
(39) Vikki, T.; RuokoLainen, J.; Ikkala, O.; Passiniemi, P.; Isotalo, H.; Torkkel, M.; Serimaa, R. *Macromolecules* **1997**, *30*, 4064. (b) Levon, K.; Ho, K.-H.; Zheng, W.-Y.; Laakso, J.; Karna, T.; Taka, T.; Osterholm, J.-E. *Polymer* **1995**, *36*, 2733.
(40) Gettinger, C. L.; Heeger, A. J.; Pine, D. J.; Cao, Y. *Synth. Met.* **1995**, *74*, 81.
(41) Ikkala, O. T.; Pietila, L.-O.; Ahjopalo, L.; Osterholm., H.; Passiniemi, P. J. *J. Chem. Phys.* **1995**, *103*, 9855. (b) Norris, I. D.; Kane-Maguire, L. A. P.; Wallace, G. G. *Macromolecules* **1998**, *31*, 6529.

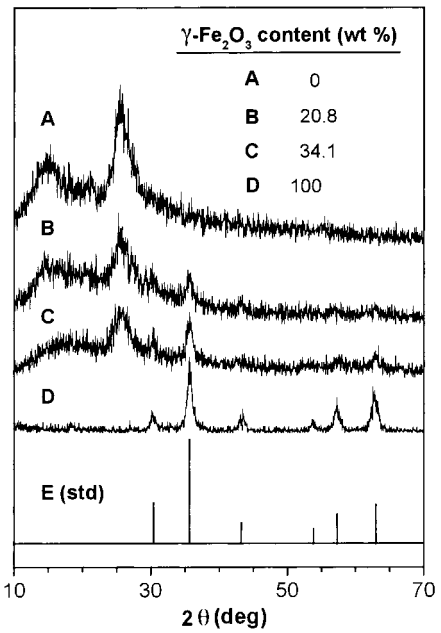

Figure 3. X-ray diffraction patterns of (A) polyaniline, (B, C) γ-Fe_2O_3−DBSA/PAn−CSA nanocomposites, and (D) γ-Fe_2O_3 nanoparticles. The vertical lines in part E are the reference data for the γ-Fe_2O_3 standard (std) taken from powder diffraction file 39-1346 of the Database of the International Center for Diffraction Data (ICDD).

surviving all the manipulations including the repeated deep cooling cycles down to 1.8 K. The mechanical strength of the films with γ-Fe_2O_3 contents higher than 50%, however, dramatically drops. The films with very high γ-Fe_2O_3 contents can be fabricated but they are too fragile to be of any practical value.

The morphology of the γ-Fe_2O_3/PAn nanocomposites is investigated by X-ray diffraction.[42] Figure 3 shows the XRD patterns of the γ-Fe_2O_3−DBS/PAn−CSA nanocomposites, as well as those of the parent PAn powders and γ-Fe_2O_3 nanoparticles. The pure PAn powders exhibit a few broad peaks at 2θ angles around 15°, 21°, and 26°. The peaks become broader and weaker when 20.8% γ-Fe_2O_3 is incorporated into PAn (Figure 3B), possibly because the nanoparticles have acted as "impurities" to hamper the growth of the PAn "crystallites".[43] A few new reflection peaks, albeit relatively weak, appear in the high-angle region of the XRD diagram of the nanocomposite. When the γ-Fe_2O_3 content further increases to 34.1%, the "peaks" of the PAn in the low-angle region become even more diffuse, while the reflections at the high angles become more visible. The parent nanoparticles display several relatively strong reflection peaks in the 2θ region of 30−70°, and it thus becomes clear that the peaks of the nanocomposites in the corresponding 2θ angles are the Bragg reflections of the iron oxide nanocrystals. The XRD patterns shown in Figure 3D are similar to those of the γ-Fe_2O_3 nanocrystals reported by other groups,[13c,14a,21,22a,44] and are in agreement with the authentic data for γ-Fe_2O_3 crystals in the ICCD Database (illustrated as vertical lines in Figure 3E), confirming that the iron oxide nanoparticles we prepared in this study are the γ-Fe_2O_3 nanocrystals of spinel structure.

Because of the extremely small dimensions of the γ-Fe_2O_3 nanocrystals, all the Bragg reflection peaks at the 2θ angles of 30.1° (d = 2.966 Å), 35.6° (2.520 Å), 43.4° (2.083 Å), 53.6° (1.708 Å), 57.3° (1.608 Å), and 62.8° (1.478 Å) are relatively broad. The average diameters (D) of the nanoparticles can be estimated by the line broadening using Scherrer formula (eq 2). The shape factor k in eq 2 is related to several aspects including shape of the crystals and Miller index of the reflecting crystallographic planes.[45] When the shape is unknown, k is often assigned a value of 0.89.[43,46] The D value associated with the strongest (311) reflection of the parent γ-Fe_2O_3 nanoparticles at $2\theta = 35.6°$ (Figure 3D) is estimated from eq 2 to be 12.0 nm, in good agreement with the average size (∼10 nm) obtained from the TEM measurements (cf., Figure 1). The D value of the nanoparticles in the nanocomposite containing 20.8% of γ-Fe_2O_3 is 10.3 nm, about 2 nm smaller than the parent form. The size further decreases to 8.0 nm when the γ-Fe_2O_3 content increases to 34.1%. Clearly, the surfactant coating has effectively sequestered the nanoclusters from aggregating during the formation of the nanocomposites. The decrease in D value may be due to the stripping of the surface layers caused by the dissolution of the initially anionic outer shells of the iron oxide nanoparticles by the protons of the surfactant acids in the early stage of the coating process, as depicted in Chart 1.

Electrical Conductivity. Electrical conductivity of the γ-Fe_2O_3−PEOPA/PAn−PEOPA and γ-Fe_2O_3−DBSA/PAn−CSA nanocomposite films is measured by the collinear four-probe technique,[28] while that of the γ-Fe_2O_3−DBSA/PAn−DBSA is not evaluated because of the poor quality of the nanocomposite films (vide ante). The conductivity of the γ-Fe_2O_3−PEOPA/PAn−PEOPA films cast from the NMP solutions is relatively low at room temperature and sharply decreases from ∼70 K. We have previously reported that PAn−CSA films cast from NMP solutions show conductivity of 10^{-3}−10^{-2} S/cm at room temperature.[28b] It is thus clear that changing the dopant (from CSA to PEOPA) and incorporating the nanoparticles do not greatly affect the conductivity of the PAn films cast from NMP solutions.

The γ-Fe_2O_3−DBSA/PAn−CSA nanocomposite films cast from the chloroform/*m*-cresol solutions, however, show much higher conductivity, probably because the well-extended polyelectrolytic conjugation conformation of the doped PAn in the mixture solutions is retained

(42) Kong, X.; Tang, B. Z. *Chem. Mater.* **1998**, *10*, 3352. (b) Tang, B. Z.; Kong, X.; Wan X.; Peng, H.; Lam, W. Y.; Feng, X.-D.; Kwok, H. S. *Macromolecules* **1998**, *31*, 2419. (c) Kong, X.; Wan, X.; Kwok, H. S.; Feng, X.-D.; Tang, B. Z. *Chin. J. Polym. Sci.* **1998**, *16*, 185. (d) Kong, X.; Lam, J. W. Y.; Tang, B. Z. *Macromolecules* **1999**, *32*, 1722.

(43) Pouget, J. P.; Jozefowicz, M. E.; Epstein, A. J.; Tang, X.; MacDiarmid, A. G. *Macromolecules* **1991**, *24*, 779. (b) Moon, Y. B.; Cao, Y.; Smith, P.; Heeger, A. J. *Polym. Commun.* **1989**, *30*, 196. (c) Wang, F.; Jingsong, T.; Wang, L.; Hongfang, Z.; Mo, Z. *Mol. Cryst. Liq. Cryst.* **1988**, *160*, 175.

(44) Kobayashi, Y.; Kawashima., D.; Tomita, A. *Chem. Mater.* **1997**, *9*, 1887. (b) del Monte, F.; Morales, M. P.; Levy, D.; Fernandez, A.; Ocana, M.; Roig, A.; Molins, E.; O'Grady, K.; Serna, C. J. *Langmuir* **1997**, *13*, 3627.

(45) Klong, H. P.; Alexander, L. E. *X-ray Diffraction Procedures for Crystalline and Amorphous Solid*; Wiley: New York, 1954. (b) Guinier, A. *Theorie et Technique de la Radio-Crystallographie*; Dunod: Paris, 1950.

(46) Kawai, H. In *Kobunshi Kagaku Joron (Introduction to Polymer Chemistry)*, 2nd ed.; Okamura, S., Nakajima, A., Onogi, S., Kawai, H., Nishijima, Y., Higashimura, T., Ise, N., Eds.; Kagaku Dojin: Kyoto, 1994; Chapter 3, pp 71−133.

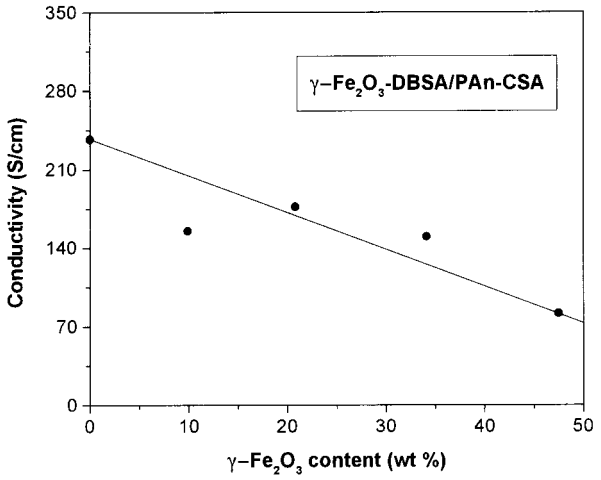

Figure 4. Effect of γ-Fe_2O_3 content on electrical conductivity of maghemite/polyaniline nanocomposite films at room temperature.

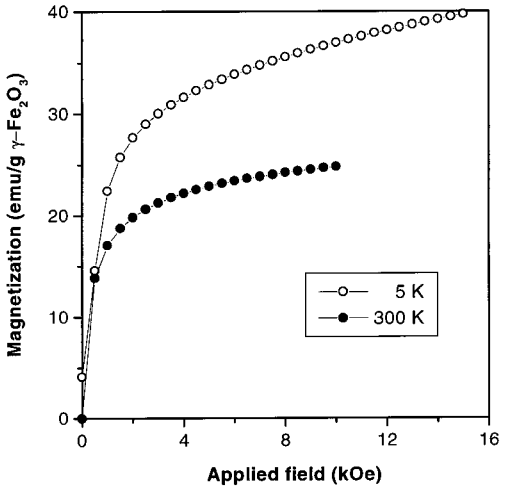

Figure 5. Magnetization curves at 5 and 300 K for γ-Fe_2O_3−DBSA/PAn−CSA nanocomposite film containing 20.8 wt % of γ-Fe_2O_3 nanoparticles.

in the solid films.[28b] As shown in Figure 4, the conductivity of the nanocomposite film decreases with increasing γ-Fe_2O_3 content. While the parent PAn−CSA film (containing no nanoparticles) cast from the chloroform/*m*-cresol solution is very conductive (237 S/cm), the conductivity of the nanocomposite film with a γ-Fe_2O_3 content of 20.8% decreases to ~180 S/cm. The decrease in conductivity may be due to partial blockage of conduction path by the γ-Fe_2O_3 nanoparticles embedded in the PAn matrix. It is, however, worth pointing out that the conductivity values of the nanocomposite films are considerably higher than those reported in the literature for other iron oxide/conducting polymer nanocomposites.[20−22,24] For example, although the γ-Fe_2O_3 content of a γ-Fe_2O_3−DBSA/PAn−CSA nanocomposite film is as high as 47.5%, its conductivity is still 82 S/cm. This is much higher than that ($\sim 10^{-4}$ S/cm) of the Fe_3O_4/PAn nanocomposite prepared by Wan et al. (although its Fe_3O_4 content was as low as ~0.01%),[24] and also higher than that (1.9 S/cm) of the γ-Fe_2O_3−(Chrome Azurol S)/PPy nanocomposite prepared by Bidan et al. with a γ-Fe_2O_3 content of 21.3%.[22]

Magnetic Susceptibility. Because of the high electrical conductivity of the γ-Fe_2O_3−DBSA/PAn−CSA nanocomposite films, we concentrated our efforts on investigating their magnetic properties.

An ultrafine particle with a diameter ≤30 nm can be seen as a magnetic monodomain, whose magnetic moment is much bigger than that of a single molecule.[22] Application of magnetic field will align the magnetic moment of the nanoparticle in the field direction, and magnetization rises with increasing field until, in many cases, a saturation value is reached. When a magnetic field is applied to the γ-Fe_2O_3/PAn nanocomposite film at 300 K, the magnetization increases rapidly without saturation and reaches 25 emu/g γ-Fe_2O_3 at an applied field of 10 kOe (Figure 5). Similarly, the magnetization of the nanocomposite increases with increasing field at 5 K. In this case again, the magnetization continuously increases without saturation. The maximum magnetization at the low temperature is 40 emu/g γ-Fe_2O_3, which is higher than that (25 emu/g γ-Fe_2O_3) of the nanocomposite at room temperature but is still lower than the saturation magnetization (74 emu/g) of the bulk γ-Fe_2O_3.[47]

The weaker magnetization and lack of saturation have often been observed in the γ-Fe_2O_3 nanoparticles of similar sizes due to the surface and size effects.[21,22a,30a,44b] The discontinuity of the superexchange bonds between the iron cations near/on the nanoparticle surfaces leads to the formation of canted spins. The noncollinear spin structure due to the pinning of the surface spins at the interface of the magnetic nanoparticles and the surfactant coating reduces the total magnetic moment of the nanoparticles and gives rise to the decrease in the magnetization of the nanocomposite films. The distribution in the nanoparticle size and the persistence of superparamagnetic relaxation of the smaller particles in the distribution leads to the nonsaturation of the magnetization.

In bulk, γ-Fe_2O_3 is a ferrimagnet. As the particles become smaller, a critical size is reached at which the bulk magnetic characteristics vanish. Such particles are called superparamagnetic and are in a state in which the direction of magnetization flips due to thermal activation. As shown in the upper panel of Figure 6, at 300 K, the magnetization vs applied field data are perfectly superimposable as the field is cycled between −5 and 5 kOe. There is no hysteresis at room temperature. Both remanence (M_r) and coercivity (H_c) are zero, consistent with the superparamagnetic behavior and the nanoscale dimensions of the particles. The particles have very small volumes, and thermal fluctuations are sufficient to overcome the anisotropy energy barrier, allowing the magnetization to spontaneously reverse direction.

As the temperature is lowered to 5 K, the magnetization increases and a hysteresis loop appears. At the low temperature, the moment of the nanoparticles with larger volumes and therefore longer relaxation times remain "frozen" in the direction of the former external field. The system is thus left with a net remanence magnetization that decays very slowly compared to the time scale of the measurement (~30 s). To bring the net magnetization to zero, a coercive magnetic field needs

(47) Hellwege, K.-K.; Hellwege, A. M. *Landolt-Börnstern: Numerical Data and Functional Relationships in Science and Technology*; Springer-Verlag: New York, 1970; New Series, Group III, Vol. 4, Part a, Figure 59.

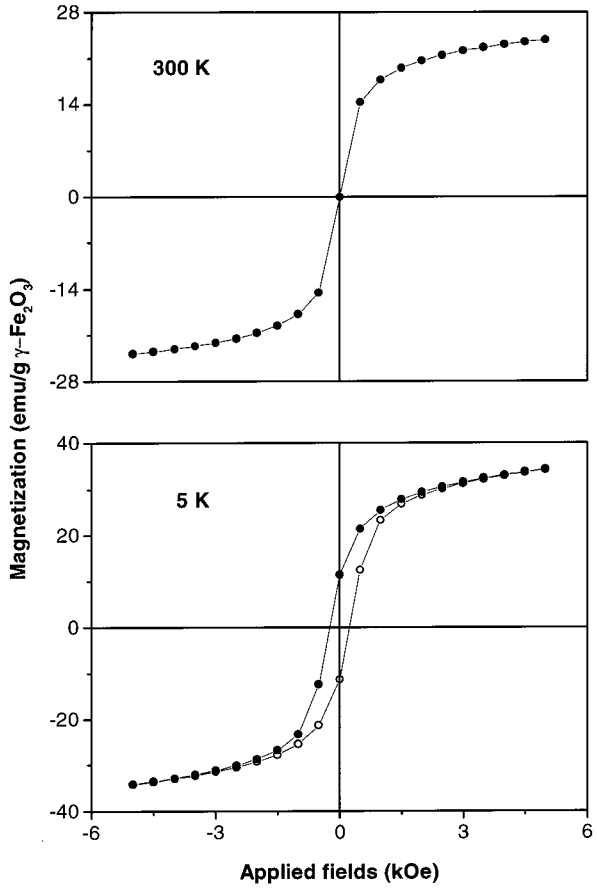

Figure 6. Magnetization vs applied field plots at 300 and 5 K for γ-Fe_2O_3−DBSA/PAn−CSA nanocomposite film containing 20.8 wt % of γ-Fe_2O_3 nanoparticles.

to be applied. Typical H_c values for bulk γ-Fe_2O_3 range from 250 to 400 Oe.[30] At the low temperature (5 K), the γ-Fe_2O_3/PAn nanocomposite film exhibits an H_c of 250 Oe and an M_r of 10.9 emu/g, similar to those (H_c = 300 Oe, M_r = 10 emu/g) reported by Kroll et al. for their nanocomposite gel of γ-Fe_2O_3/alginate (a polysaccharide) at the same temperature.[14a]

A commonly used technique for the investigation of superparamagnetic relaxation is the field-cooled (FC) and zero-field-cooled (ZFC) magnetization, that is, the magnetization in a weak applied field as a function of increasing temperature after the sample has been cooled respectively in the presence and absence of a weak magnetic field. Figure 7 shows the FC and ZFC data of the γ-Fe_2O_3/PAn nanocomposite film in a weak magnetic field of 50 Oe. At high temperatures, the two sets of data exhibit the same trend; that is, the magnetization decreases with increasing temperature. At low temperatures, however, the data significantly diverge. The magnetization increases monotonically with decreasing temperature in the FC case, indicative of the presence of ultrafine superparamagnetic particles in the nanocomposite film. The ZFC magnetization curve, however, separates from the FC curve and passes through a maximum at 125 K (T_{max}).

According to Neel's theory and its generalization by Brown, for particles of volume V, there exists a critical temperature T_b, called blocking temperature.[48] At a temperature $T > T_b$, the thermal energy is comparable to the magnetic energy barrier. The spins in the magnetic domain are thermally excited to fluctuate

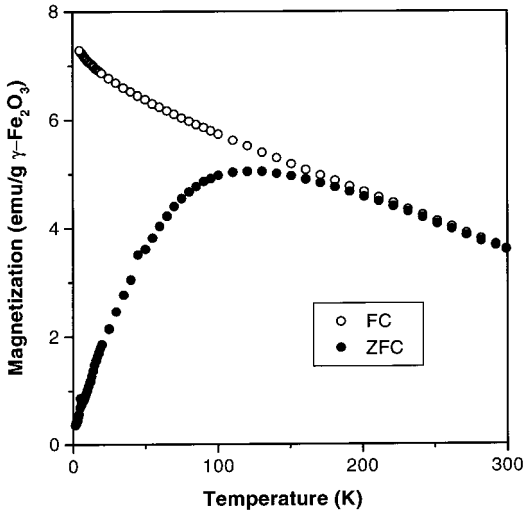

Figure 7. Temperature dependence of magnetization in a field of 50 Oe for γ-Fe_2O_3−DBSA/PAn−CSA nanocomposite film containing 20.8 wt % of γ-Fe_2O_3 nanoparticles. The field-cooled (FC) and zero-field-cooled (ZFC) curves correspond to the samples freezing, respectively, with and without applying the magnetic field prior to the magnetization measurements.

between the easy directions of magnetization. When $T < T_b$, the moments of the particles of all sizes smaller than the critical volume V_c for that temperature are magnetically frozen along their anisotropy axes, and the thermodynamic equilibrium is "blocked". The ZFC magnetization exhibits a maximum at the temperature T_{max} at which the (average) relaxation time equals the time scale of magnetization measurement. T_{max} is related to T_b by eq 3, where the β value changes with the shape of the size distribution curve of the particles.[49] For the monodisperse particles (i.e., all particles possessing the same size), β is unity and $T_{max} = T_b$. For the particles with size distributions, β is typically in the range of 1.5−2.0[22b,30c,49,50] and T_b is now the blocking temperature for the particles with an *average* volume. The maximum of the ZFC curve in Figure 7 is thus associated with the T_b of the γ-Fe_2O_3/PAn nanocomposite. The broadness of the peak maximum of the ZFC curve as well as the TEM image in Figure 1 clearly shows that the nanoparticles are polydisperse in size. It is thus estimated from eq 3 that T_b for the nanocomposite is in the temperature region of 63−83 K.

Conclusions

The previous efforts in the preparation of iron oxide/conducting polymer nanocomposites have often ended up with intractable products with low conductivity being obtained. In this work, we developed a versatile process for the preparation of γ-Fe_2O_3/PAn nanocomposite films. Our approach employing the anionic surfactants enables (i) coating/stabilization of the γ-Fe_2O_3 nanoparticles, (ii) dissolution of the PAn chains, (iii) doping of the emer-

(48) Neel, L. *Rev. Mod. Phys.* **1953**, *25*, 293. (b) Neel, L. *Adv. Phys.* **1955**, *4*, 191. (c) Brown, W. F., Jr. *Fluctuation Phenomena in Solids*; Academic: New York, 1964. (d) Cullity, B. D. *Introduction to Magnetic Materials*; Addison-Wesley: Reading, MA, 1972.

(49) El-Hilo, M.; O'Grady, K.; Chantrell, R. W. *J. Magn. Magn. Mater.* **1992**, *114*, 295. (b) Chantrell, R. W.; El-Hilo, M.; O'Grady, K. *IEEE Trans. Magn.* **1991**, *27*, 3570. (c) Gittleman, J. I.; Abeles, B.; Bozoeski, S. *Phys. Rev. B* **1974**, *9*, 3891.

(50) El-Hilo, M.; O'Grady, K. *IEEE Trans. Magn.* **1990**, *26*, 1807.

aldine base without using destructive acids such as HCl, (iv) amalgamation of γ-Fe_2O_3 and PAn in common solvents, (v) fabrication of free-standing nanocomposite films by static casting, and (vi) manipulation of the γ-Fe_2O_3 content and film thickness by changing the γ-Fe_2O_3/PAn ratio and concentration. The γ-Fe_2O_3−DBSA/PAn−CSA nanocomposite films show electrical conductivity ($\sigma = 82-237$ S/cm) much higher than that of the iron oxide/conducting polymer systems reported in the literature (3.4×10^{-7} to 1.9 S/cm).[20−24] The nanocomposite films are superparamagnetic, showing no hysteresis loop at 300 K and exhibiting a T_b in the temperature region of 63−83 K.

The γ-Fe_2O_3/PAn nanocomposites we prepared in this work thus have the following noteworthy features: they are macroscopically processible, electrically conductive, and magnetically susceptible. Such attractive features make the nanocomposites promising candidates for advanced materials to be used in the high-technology industries. Noticing that the doping of PAn by CSA can generate chiral emeraldine salts,[35a,41b,51] the γ-Fe_2O_3−DBSA/PAn−CSA nanocomposites should also be optically active and may find potential applications in such areas as asymmetric synthesis, chiral chromatography, and membrane enantioseparation.[52] Work on the exploration of such applications is currently under way in our laboratories and will be published in due course.

Acknowledgment. This project was partially supported by the Joint Laboratory for Nanostructured Materials and Technology between HKUST and CAS. We thank Professor Ping Sheng, Director of the Joint Laboratory, for his valuable and stimulating discussions. This project also benefited from the financial support from the Research Grants Council of the Hong Kong Special Administrative Region, China (Project Nos. HKUST6062/98P and HKUST6111/98P).

CM9900305

(51) Minto, C. D. G.; Vaugham, A. S. *Polymer* **1996**, *37*, 359. (b) Havinga, E. E.; Bouman, M. M.; Meijer, E. W.; Pomp, A. A.; Simenon, M. M. J. *Synth. Met.* **1994**, *35*, 93.

(52) Tang, B. Z.; Wan, X.; Kwok, H. S. *Eur. Polym. J.* **1998**, *34*, 341. (b) Tang, B. Z. *Adv. Mater.* **1990**, *2*, 107. (c) Tang, B. Z.; Kotera, N. Jpn. Patent H2-258807, 1990. (d) Tang, B. Z.; Kotera, N. *Macromolecules* **1989**, *22*, 4388. (e) Sun, Q.; Tang, B. Z. *Polym. Prepr.* **1999**, *40*, 560.